Submitted to the
International Europhysics Conference on High Energy Physics
Aachen, Germany, July 17 – 23, 2003

Abstract: 524 **Session: HP, NPFT**

Observation of $K^0_s K^0_s$ resonances in deep inelastic scattering at HERA

ZEUS Collaboration

17. July 2003

Abstract

Inclusive $K^0_s K^0_s$ production in deep inelastic ep scattering at HERA has been studied with the ZEUS detector using an integrated luminosity of 120 pb^{-1}. Two states are observed at masses of 1537^{+9}_{-8} MeV and 1726^{+7}_{-7} MeV, as well as an enhancement around 1300 MeV. The state at 1537 MeV is consistent with the well established $f'_2(1525)$. The state at 1726 MeV may be the glueball candidate $f_0(1710)$.

1 Introduction

The $K_s^0 K_s^0$ system is expected to couple to scalar and tensor glueballs. This has motivated intense experimental and theoretical study during the past few years [1, 2]. Lattice QCD calculations [3] predict the existence of a scalar glueball with a mass of 1730 ± 100 MeV and a tensor glueball at 2400 ± 120 MeV. The scalar glueball can mix with $q\overline{q}$ states with $I = 0$ from the scalar meson nonet, leading to three $J^{PC} = 0^{++}$ states whereas only two can fit into the nonet. Experimentally, four states with $J^{PC} = 0^{++}$ and $I = 0$ have been established [4]: $f_0(980)$, $f_0(1370)$, $f_0(1500)$ and $f_0(1710)$.

The state most frequently considered to be a glueball candidate is $f_0(1710)$ [4], but its gluon content has not yet been established. This state was first observed in radiative J/ψ decays [5] and its angular momentum $J = 0$ was established by the WA102 experiment using a partial-wave analysis in the K^+K^- and $K_s^0 K_s^0$ final states [6]. Observation of $f_0(1710)$ in $\gamma\gamma$ collisions may indicate a large quark content. A recent publication from L3 [7] reports the observation of two states in $\gamma\gamma$ collisions above 1500 MeV, the well-established $f_2'(1525)$ [4] and a broad resonance at 1760 MeV. It is not clear if this state is the $f_0(1710)$.

The ep collisions at HERA provide an opportunity to study resonance production in a new environment. The production of K_s^0 has been studied previously at HERA [8, 9]. In this paper, the first observation of resonances in the $K_s^0 K_s^0$ final state in inclusive ep deep inelastic scattering (DIS) is reported.

2 Experimental set-up

The data were collected by the ZEUS detector at HERA during the 96-00 running periods. In 96-97, HERA collided 27.5 GeV positrons with 820 GeV protons. In 98-00, the proton energy was increased to 920 GeV and positrons or electrons were collided. The measurements for e^+p (e^-p) interactions[1] are based on an integrated luminosity of $104\,\mathrm{pb}^{-1}$ ($17\,\mathrm{pb}^{-1}$).

A detailed description of the ZEUS detector can be found elsewhere [10]. A brief outline of the components that are most relevant for this analysis is given below.

Charged particles are tracked in the central tracking detector (CTD) [11], which operates in a magnetic field of 1.43 T provided by a thin superconducting solenoid. The CTD consists of 72 cylindrical drift chamber layers, organized in nine superlayers covering the

[1] Hereafter, both e^+ and e^- are referred to as electrons, unless explicitly stated otherwise.

polar-angle[2] region $15^\circ < \theta < 164^\circ$. The relative transverse-momentum resolution for full-length tracks is $\sigma(p_T)/p_T = 0.0058 p_T \oplus 0.0065 \oplus 0.0014/p_T$, with p_T in GeV. The tracking system was used to establish the primary and secondary vertices.

The high-resolution uranium–scintillator calorimeter (CAL) [12] consists of three parts: the forward (FCAL), the barrel (BCAL) and the rear (RCAL) calorimeters. Each part is subdivided transversely into towers and longitudinally into one electromagnetic section (EMC) and either one (in RCAL) or two (in BCAL and FCAL) hadronic sections (HAC). The smallest subdivision of the calorimeter is called a cell. The CAL energy resolutions, as measured under test-beam conditions, are $\sigma(E)/E = 0.18/\sqrt{E}$ for electrons and $\sigma(E)/E = 0.35/\sqrt{E}$ for hadrons, with E in GeV.

The energy of the scattered electron was corrected for energy loss in the material between the interaction point and the calorimeter using a small-angle rear tracking detector (SRTD) [13, 14] and a presampler (PRES) [14, 15].

3 Kinematic reconstruction and event selection

The inclusive neutral current DIS process $e(k) + p(P) \rightarrow e(k') + X$ can be described in terms of the following variables: the negative of the invariant-mass squared of the exchanged virtual photon $Q^2 = -q^2 = -(k - k')^2$, the fraction of the lepton energy transferred to the proton in the proton rest frame $y = (q \cdot P)/(k \cdot P)$, and the Bjorken scaling variable $x = Q^2/(2P \cdot q)$.

A three-level trigger system was used to select events online [10]. The inclusive DIS selection was defined by requiring an electron found in the CAL. In certain run periods, corresponding to 83% of the total luminosity, the inclusive selection was not available for low Q^2 ($Q^2 < 20$ GeV^2) events. For these events, an additional selection with a requirement of at least one forward jet identified with the k_t algorithm [16] and having transverse energy $E_T > 3$ GeV ($E_T > 4$ GeV in the 2000 running period), pseudorapidity $0 < \eta_{\rm jet} < 3$ ($1.5 < \eta_{\rm jet} < 3.5$ in the 1996-1997 running period) was used.

The DIS offline event selection is based on the following requirements:

- a primary vertex position, determined from the tracks fitted to the vertex, in the range $|\, Z_{\rm vertex} \,| < 50$ cm, to reduce the background events from non-ep interactions;

[2] The ZEUS coordinate system is a right-handed Cartesian system, with the Z axis pointing in the proton beam direction, referred to as the "forward direction", and the X axis pointing left towards the centre of HERA. The coordinate origin is at the nominal interaction point. The pseudorapidity is defined as $\eta = -\ln\left(\tan\frac{\theta}{2}\right)$, where the polar angle, θ, is measured with respect to the proton beam direction.

- $E_e \geq 8.5$ GeV, where E_e is the energy of the scattered electron reconstructed in the calorimeter;
- $42 < \delta < 60$ GeV, where $\delta = \sum E_i(1 - \cos\theta_i)$, E_i is the energy of the i^{th} calorimeter cell and θ_i is its polar angle as viewed from the primary vertex. The sum runs over all cells. This cut further reduces the background from photoproduction and events with large QED initial-state radiation;
- $y_e \leq 0.95$, to remove events with misidentified scattered DIS electrons; y_e is the value of y reconstructed using the scattered electron measurement;
- $y_{JB} \geq 0.04$, to remove events with low hadronic activities; y_{JB} is the value of y reconstructed using the Jaquet-Blondel method [17];
- the position of the scattered lepton candidate in the RCAL was required to be outside a box of ± 14 cm in X and Y, which corresponds approximately to $\theta_{ele} \approx 176^o$, where θ_{ele} is the polar angle of the scattered electron;
- a maximum of 40 tracks per event. This cut reduces the background from false K_s^0 pair candidates, removing 7% of the DIS events.

The non-ep and photoproduction background in the selected sample was estimated to be negligible. The data were not corrected for the biases introduced by the trigger requirements and selection cuts.

4 Selection of K_s^0 pair candidates

Only oppositely charged track pairs with at least 38 hits in the CTD and assigned to a secondary vertex were selected and combined to form K_s^0 candidates. Both tracks were assigned the mass of a charged pion and the invariant-mass $M(\pi^+\pi^-)$ was calculated. Events with at least two K_s^0 candidates and $-1.75 < \eta_\pi < 1.75$, where η_π is the pseudorapidity of each pion, were selected. The η_π cut and the required minimum number of hits ensure a good momentum resolution. The secondary vertex resolution for these events, estimated using MC studies, is 2 mm in X and Y, and 4 mm in Z.

Additional requirements were applied to the selected K_s^0 candidates:

- $p_T(K_s^0) > 200$ MeV, for each K_s^0 candidate;
- $2 < d < 30$ cm, where d is the decay length of the K_s^0 candidate;
- $d_{XY} < 4$ mm and $d_Z < 5.5$ mm, where d_{XY} and d_Z are, respectively, the projections on the XY plane and Z axis of the vector defined by the primary interaction point and the point of closest approach of the K_s^0 candidate;

- $\theta_{XY} < 0.12$, where θ_{XY} is the (collinearity) angle between the candidate K^0_s momentum vector and the vector defined by the interaction point and the K^0_s decay vertex in the XY plane;
- $p_T^A > 110$ MeV, for each K^0_s candidate, where the Armenteros-Podolanski variable p_T^A is the projection of the candidate pion momentum onto a plane perpendicular to the K^0_s candidate line of flight [18].

The cuts on the decay length, distance of closest approach and collinearity angle significantly reduce the non-K^0_s background as determined by Monte Carlo (MC) simulations. After the p_T^A cut, backgrounds from Λ, $\overline{\Lambda}$ and photon conversions are negligible.

Figure 1 shows the invariant-mass distribution for K^0_s candidates in the range $0.45 < M(\pi^+\pi^-) < 0.55$ GeV after the K^0_s pair candidate selection. The distribution was fitted using one linear and two Gaussian functions. The linear function fits the background, one of the Gaussians fits the peak region in the central $\pi^+\pi^-$ invariant mass distribution, and the other Gaussian improves the fit at the tails. The two Gaussians are constrained to have the same mean value. A mass of 498 MeV and standard deviation of 4 MeV are obtained from the fit with the central Gaussian, and a standard deviation of 8.5 MeV is obtained from the fit with the other Gaussian. The normalization factor between the narrower and broader Gaussians is approximately 5.5. The invariant-mass width is dominated by the momentum resolution of tracks reconstructed with the CTD. Only K^0_s candidates in the region of ± 10 MeV around the fitted central mass were used to reconstruct the $K^0_s K^0_s$ invariant-mass.

Figure 2 shows the distribution in x and Q^2 of selected events containing at least one pair of K^0_s candidates. The kinematic variables were reconstructed using the double angle method [19]. The virtual photon-proton centre-of-mass energy was in the range $50 < W < 250$ GeV.

5 Results

The $K^0_s K^0_s$ spectrum may have a strong enhancement near the $K^0_s K^0_s$ threshold due to the $f_0(980)/a_0(980)$ state [20, 21]. Since the high $K^0_s K^0_s$ mass is the region of interest for this analysis, the complication due to the threshold region is avoided by requiring the cut $cos\theta_{K^0_s K^0_s} < 0.92$, where $\theta_{K^0_s K^0_s}$ is the opening angle between the two K^0_s candidates in the laboratory frame.

After applying all selection cuts, 2553 K^0_s pair candidates were found in the range $0.995 < M(K^0_s K^0_s) < 2.795$ GeV, where $M(K^0_s K^0_s)$ is calculated using the K^0_s mass of 497.672 MeV [4]. The momentum resolution of the CTD leads to an average $M(K^0_s K^0_s)$ resolution which

ranges from 7 MeV in the 1300 MeV mass region to 10 MeV in the 1700 MeV region. Figure 3 shows the measured $K^0_s K^0_s$ invariant-mass spectrum. Two clear peaks are seen, one around 1500 MeV and the other around 1700 MeV, along with an enhancement around 1300 MeV. The data for $cos\theta_{K^0_s K^0_s} > 0.92$ are also shown.

The distribution shown in Fig. 3 was fitted using three modified relativistic Breit-Wigner (MRBW) distributions and a background function $U(M)$;

$$F(M) = \sum_{i=1}^{3} \left(\frac{m_{*,i}\Gamma_{d,i}}{(m^2_{*,i} - M^2)^2 + m^2_{*,i}\Gamma^2_{d,i}}\right) + U(M) \ , \tag{1}$$

where $\Gamma_{d,i}$ is the effective resonance width that takes into account spin and large width effects [22], $m_{*,i}$ is the resonance mass, and M is $K^0_s K^0_s$ invariant mass. The background function is

$$U(M) \ = \ A \cdot (M - 2m_{K^0_s})^B \cdot e^{-C\sqrt{M-2m_{K^0_s}}} \ , \tag{2}$$

where A, B and C are free parameters and $m_{K^0_s}$ is the K^0_s mass from [4].

Below 1500 MeV, a region strongly affected by the $cos\theta_{K^0_s K^0_s}$ cut, a peak is seen around 1300 MeV where a contribution from $f_2(1270)/a^0_2(1320)$ is expected. This mass region was fitted with a single Breit-Wigner.

Above 1500 MeV, the lower-mass state has a fitted mass of 1537^{+9}_{-8} MeV and a width of 50^{+34}_{-22} MeV in good agreement with the well-established $f'_2(1525)$. The higher-mass state has a fitted mass of 1726 ± 7 MeV and a width of 38^{+20}_{-14} MeV. The widths reported here are stable to a wide variation of fitting methods within statistical errors. The width is narrower than the PDG value (125 ± 10 MeV) [4] reported for $f_0(1710)$ but when it is fixed to this value the fit is still acceptable. For the purposes of the following discussion we refer to this state as $f_0(1710)$.

The masses, widths and number of events from the fit with statistical errors are given in the top row of Table 1. The mass spectrum is also consistent with the background function at higher masses, but is not included in the fit due to limited statistics. The sensitivity of the data to the widths of the resonances was studied. Several fits were performed fixing the width of the states $f'_2(1525)$ and $f_0(1710)$ to their PDG values and the results are shown in rows 2 to 4 of Table 1.

In the literature, there are several states reported in the mass region near 2 GeV [4], namely $f_2(1950)$ and $f_0(2020)$ which need confirmation, and $f_2(2010)$, $a_4(2040)$ and $f_4(2050)$ which have been confirmed. The effect of the inclusion of a state in this region was examined, with the result shown in row 5 of Table 1.

The $K^0_s K^0_s$ spectrum after all cuts was also fitted with the background function only. The fit can be rejected with a 99.4% confidence level using a χ^2 test.

It was found that 93% of the K^0_s pair candidates selected after all cuts are in the target region of the Breit frame [23], which corresponds to the remnant of the proton. Of these events, 78% are in the gluon-rich region $x_p = 2p_B/Q > 1$, where p_B is the absolute momentum of the $K^0_s K^0_s$ in the Breit frame.

6 Conclusions

The first observation in *ep* deep inelastic scattering of a state at 1537 MeV, consistent with $f'_2(1525)$, and another at 1726 MeV, close to $f_0(1710)$, is reported. The width of the state at 1537 MeV is consistent with the PDG value for the $f'_2(1525)$. The state at 1726 MeV has a width of 38^{+20}_{-14} MeV which is narrower than the PDG value of 125±10 MeV for the $f_0(1710)$. There is also an enhancement near 1300 MeV which may arise from the production of $f_2(1270)$ and/or $a^0_2(1320)$ states.

7 Acknowledgements

We thank the DESY directorate for their strong support and encouragement. The special efforts of the HERA machine group in the collection of the data used in this paper are gratefully acknowledged. We are grateful for the support of the DESY computing and network services. The design, construction and installation of the ZEUS detector have been made possible by the ingenuity and effort of many people from DESY and home institutes who are not listed as authors. We also thank F. Close, S. Godfrey and H. Lipkin for their invaluable comments and advice.

References

[1] S. Godfrey, J. Napolitano, Review of Modern Physics **71**, 1411 (1999).

[2] E. Klempt, Preprint hep-ex/0101031, 2000.

[3] C. J. Morningstar, M. Peardon, Phys. Rev. **D 60**, 034509 (1999);
C. Michael and M. Teper, Nucl. Phys. **B 314**, 347 (1989).

[4] K. Hagiwara et al., Phys. Rev. **D 66**, 1 (2002).

[5] J. Z. Bai et al, BES Collaboration, Phys. Rev. Lett. **77**, 3959 (1996).

[6] By WA102 Collaboration (D. Barberis et al), Phys. Lett. **B 453**, 305 (1999).

[7] By L3 Collaboration (M. Acciari et al), Phys. Lett. **B 501**, 173 (2001).

[8] ZEUS Coll., J. Breitweg et al., Eur. Phys. J. **C 2**, 77 (1998);
ZEUS Coll., M. Derrick et al., Z. Phys. **C 68**, 29 (1995).

[9] H1 Coll., S. Aid et al., Nucl. Phys. **B 480**, 3 (1996).

[10] ZEUS Coll., U. Holm (ed.), *The ZEUS Detector*. Status Report (unpublished), DESY (1993), available on `http://www-zeus.desy.de/bluebook/bluebook.html`.

[11] N. Harnew et al., Nucl. Inst. Meth. **A 279**, 290 (1989);
B. Foster et al., Nucl. Phys. Proc. Suppl. **B 32**, 181 (1993);
B. Foster et al., Nucl. Inst. Meth. **A 338**, 254 (1994).

[12] M. Derrick et al., Nucl. Inst. Meth. **A 309**, 77 (1991);
A. Andresen et al., Nucl. Inst. Meth. **A 309**, 101 (1991);
A. Caldwell et al., Nucl. Inst. Meth. **A 321**, 356 (1992);
A. Bernstein et al., Nucl. Inst. Meth. **A 336**, 23 (1993).

[13] A. Bamberger et al., Nucl. Inst. Meth. **A 401**, 63 (1997).

[14] ZEUS Coll., S. Chekanov et al., Eur. Phys. J. **C 21**, 443 (2001).

[15] A. Bamberger et al., Nucl. Inst. Meth. **A 382**, 419 (1996).

[16] S. Catani et al., Nucl. Phys. **B 406**, 187 (1993).

[17] F. Jacquet and A. Blondel, *Proceedings of the Study for an ep Facility for Europe*, U. Amaldi (ed.), p. 391. Hamburg, Germany (1979). Also in preprint DESY 79/48.

[18] J. Podolanski and R. Armenteros, Phil. Mag **45**, 13 (1954).

[19] S. Bentvelsen, J. Engelen and P. Kooijman, *Proc. Workshop on Physics at HERA*, W. Buchmüller and G. Ingelman (eds.), Vol. 1, p. 23. Hamburg, Germany, DESY (1992).

[20] S. Godfrey and N. Isgur, Phys. Rev. **D32**, 189 (1985).

[21] By WA102 Collaboration (D. Barberis et al), Phys. Lett. **B 489**, 24 (2000);
T. Barnes, Preprint hep-ph/0202157, 2002.

[22] J. Benecke and H. P. Dürr, Nuovo Cimento **56**, 269 (1968).

[23] R. P. Feynman, *Photon-Hadron Interactions*, Benjamin, New York, 1972;
K.H. Streng, T.F. Walsh and P.M. Zerwas, Z. Phys. **C 2**, 237 (1979).

Fit	χ^2/N	$f_2(1270)/a_2^0(1320)$			$f_2'(1525)$			$f_0(1710)$			$f_J(1980)$		
		mass	width	events	mass	width	events	mass	width	events	mass	width	events
1	0.97	1274^{+17}_{-16}	244^{+85}_{-58}	414^{+184}_{-125}	1537^{+9}_{-8}	50^{+34}_{-22}	84^{+41}_{-31}	1726^{+7}_{-7}	38^{+20}_{-14}	74^{+29}_{-23}			
2	0.96	1272^{+16}_{-16}	240^{+76}_{-55}	420^{+167}_{-122}	1539^{+10}_{-10}	76	107^{+30}_{-30}	1727^{+7}_{-7}	39^{+20}_{-20}	76^{+28}_{-24}			
3	1.02	1276^{+16}_{-16}	258^{+80}_{-59}	480^{+190}_{-141}	1536^{+8}_{-8}	49^{+30}_{-21}	85^{+38}_{-27}	1726^{+13}_{-13}	125	122^{+40}_{-40}			
4	1.02	1274^{+15}_{-15}	251^{+72}_{-55}	476^{+176}_{-131}	1538^{+10}_{-10}	76	108^{+31}_{-29}	1728^{+13}_{-13}	125	120^{+41}_{-38}			
5	1.00	1283^{+15}_{-15}	260^{+70}_{-55}	506^{+218}_{-122}	1540^{+12}_{-10}	70^{+43}_{-30}	116^{+59}_{-42}	1727^{+7}_{-7}	47^{+23}_{-15}	91^{+34}_{-26}	1970^{+33}_{-45}	138^{+173}_{-89}	74^{+40}_{-40}
Particle Data Group 2002 Values (MeV) [4]													
		1275.5 ± 1.2, $185^{+3.4}_{-2.6}$ 1318 ± 0.6, 104.7 ± 1.9			1525 ± 5, 76 ± 10			1713 ± 6, 125 ± 10					

Table 1: *Normalized χ^2, masses in MeV, widths in MeV, and number of events extracted from the $K_s^0K_s^0$ invariant-mass fits (errors were statistical only.) Widths reported without errors are fixed to the PDG values listed in the last row.*

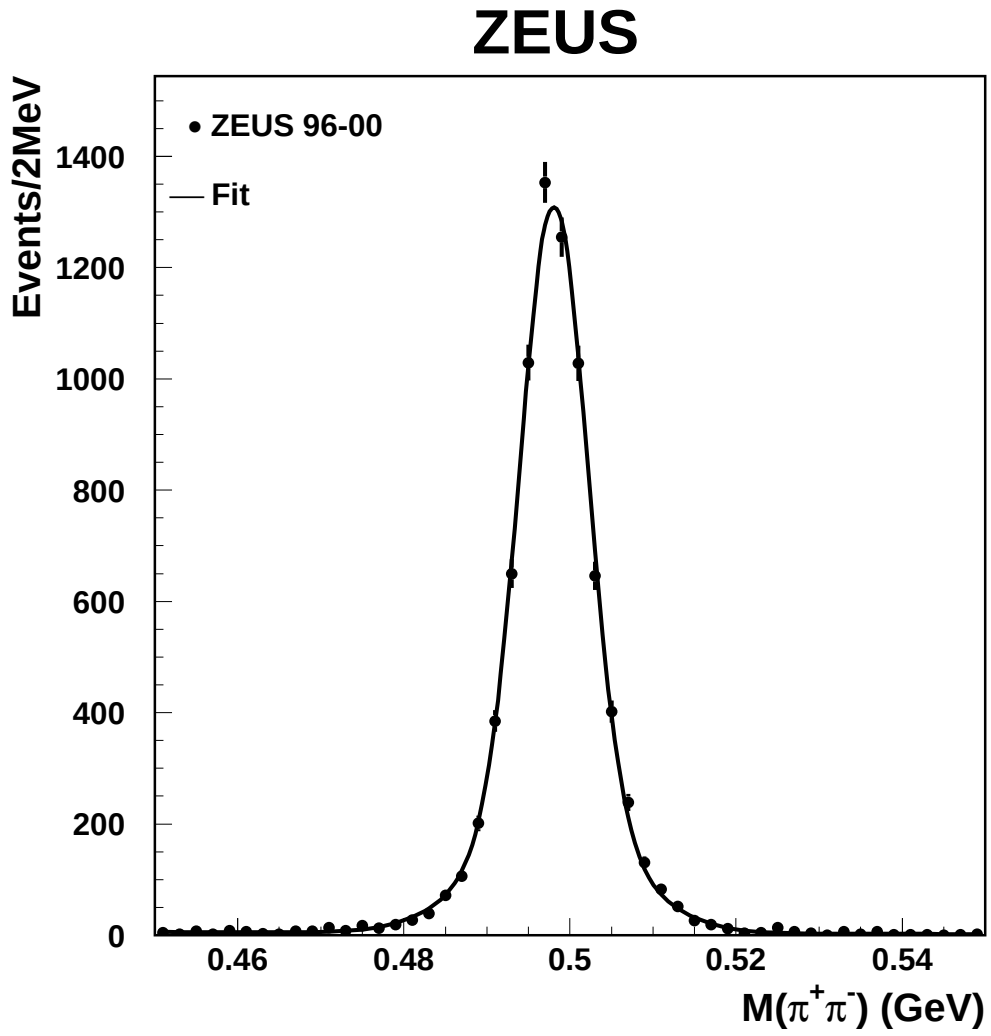

Figure 1: *The distribution of $\pi^+\pi^-$ invariant-mass for events with at least two K_s^0 candidates passing all selection cuts. The solid line shows the result of a fit using one linear and two Gaussian functions.*

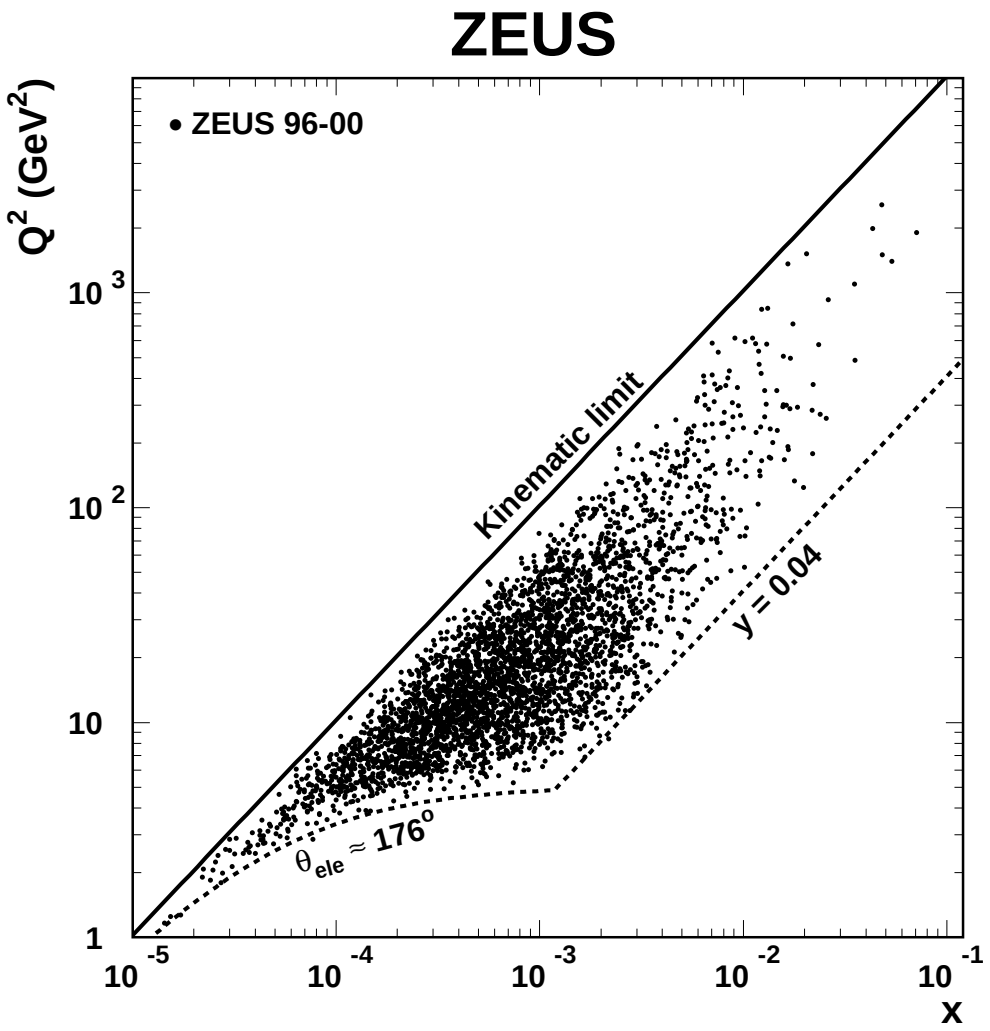

Figure 2: *The distribution in x and Q^2 of events passing all selection cuts. The dashed lines delineate approximately the kinematic region selected. The solid line indicates the kinematic limit for HERA running with 920 GeV protons.*

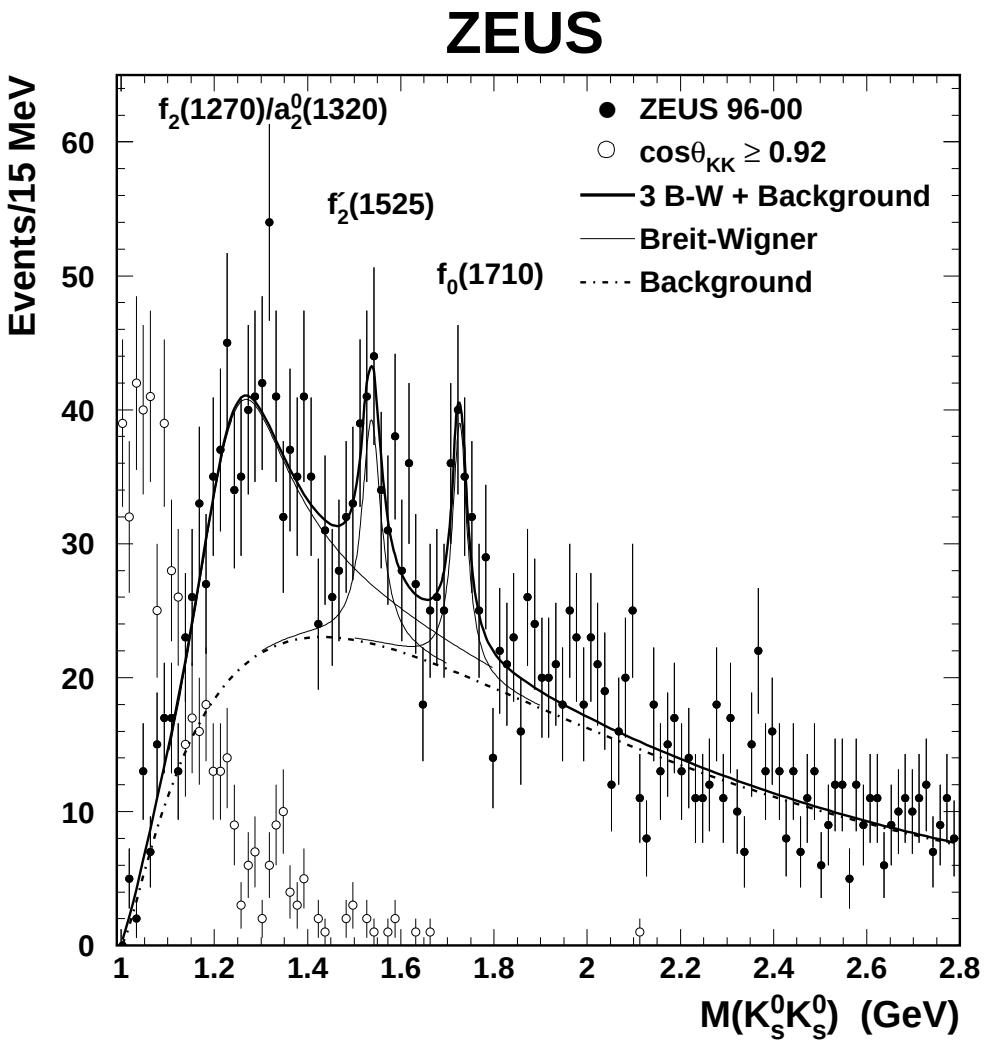

Figure 3: *The $K_s^0 K_s^0$ invariant-mass spectrum for K_s^0 pair candidates with $cos\theta_{K_s^0 K_s^0} < 0.92$ (filled circles). The thick solid line is the result of a fit using three Breit-Wigners (thin solid lines) and a background function (dotted-dashed line). The K_s^0 pair candidates that fail the $cos\theta_{K_s^0 K_s^0} < 0.92$ cut are also shown (open circles).*